Capturing Resting Cardiovascular Coupling as an Indicator of Orthostatic Hypotension using a Multimodal Chest-Worn Patch

Vikram Abbaraju ¹, John A. Berkebile ¹, Paul A. Beach ², and Omer T. Inan ¹

¹ School of Electrical and Computer Engineering, Georgia Institute of Technology, Atlanta, GA, USA
² Department of Neurology, Emory University School of Medicine, Atlanta, GA, USA

Abstract—Orthostatic hypotension (OH), caused by efferent baroreflex failure, can lead to syncope and is associated with high mortality rates among individuals with neurodegenerative diseases. Several studies in recent years have aimed to estimate baroreflex sensitivity (BRS) during orthostatic stressors using measures of cardiovascular coupling (CVC): the degree of synchronization between time series cardiovascular signals. However, these efforts have relied on blood pressure sensing using bulky, wired setups, and the majority have only quantified changes in CVC during or after the occurrence of OH. In this study, we characterized CVC at rest in N = 26 participants (20 with a neurodegenerative disease) using a chest-worn patch that recorded electrocardiogram (ECG) and photoplethysmogram (PPG) signals. From the ECG and PPG data recorded during a 5minute supine rest period prior to an orthostatic challenge, we derived interbeat interval (IBI) and PPG amplitude (PPG_{amp}) time series features as indices of cardiac rhythm and vascular function, respectively. We then quantified the coupling between IBI and PPG_{amp} using time delay stability (TDS). Following an active standing test, 12 participants experienced OH. We found that mean TDS during the rest period was 22.9% lower in the OH group than in the no-OH group (p < 0.01). Furthermore, we found that resting TDS was moderately correlated with the change in systolic blood pressure from supine to standing ($\rho = 0.43$, p <0.05). Thus, we demonstrated the effectiveness of a multimodal wearable in capturing a marker of impaired resting CVC prior to OH occurrence. This work enables the deployment of wearable sensing for estimating BRS to assist with early screening of autonomic dysfunction in the future.

Keywords—cardiovascular coupling, baroreflex sensitivity, multimodal wearable, orthostatic hypotension, neurodegenerative disease

I. INTRODUCTION

Cardiovascular autonomic dysfunction (CVAD) is a common feature of neurodegenerative synucleinopathies, including Parkinson's disease (PD), multiple system atrophy (MSA), and dementia with Lewy bodies (DLB) [1]. CVAD often manifests in orthostatic hypotension (OH), a sustained fall in systolic blood pressure (SBP) following a postural change from supine to standing [1], [2]. Clinically, OH is defined as a fall in systolic blood pressure (SBP) of at least 20 mmHg and/or a fall in diastolic blood pressure (DBP) of at least 10 mmHg within 3 minutes of upright posture [3]. OH is associated with incapacitating dizziness, syncope (fainting) and catastrophic injuries, and is an independent predictor of mortality risk, especially in the elderly population [4]. Consequently, early detection of OH—or, ideally, the risk of developing OH—is of

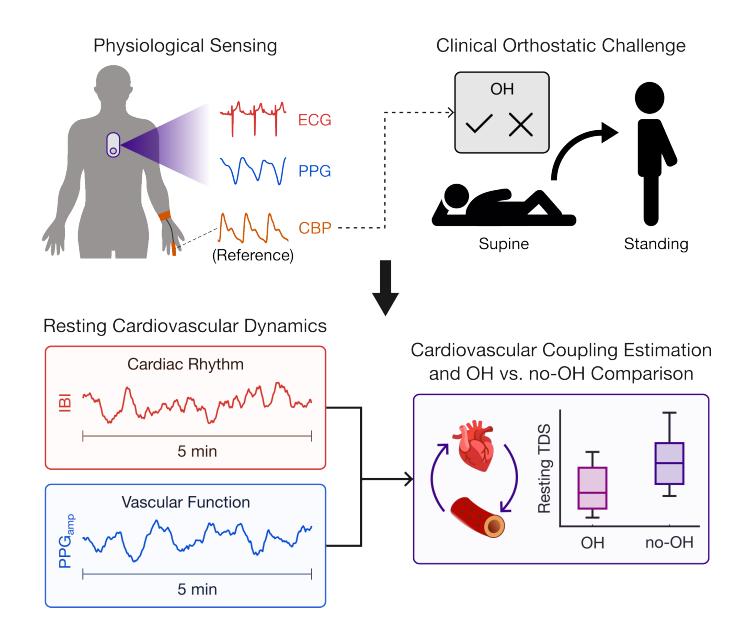


Fig. 1. Overview of the analysis presented in this work. We used a wireless chest-worn patch to record electrocardiogram (ECG) and photoplethysmogram (PPG) signals during an orthostatic challenge in N=26 participants. We also collected reference continuous (CBP) signals, from which we assessed whether each participant experienced orthostatic hypotension (OH) following the challenge. From the ECG and PPG signals during the supine rest period, we estimated time series indices of cardiac rhythm and vascular function, respectively. From these indices, we computed the degree of cardiovascular coupling during supine rest using time delay stability (TDS) and statistically compared the distribution of TDS between those who experienced OH and those who did not following the orthostatic challenge.

critical importance, particularly in the elderly and those with neurodegenerative diseases associated with autonomic failure.

Neurogenic OH is most commonly caused by failed postural blood pressure regulation due to efferent baroreflex failure [5]. Recently, several studies have estimated baroreflex sensitivity (BRS)—the relationship between changes in cardiac interbeat interval changes and subsequent changes in blood pressure—in those with OH using signal processing techniques that quantify changes in *cardiovascular coupling* (CVC). These techniques entail computing the degree of synchronization or information transfer between interbeat interval (IBI) and SBP time series during different phases of an orthostatic challenge [6]–[8]. However, most prior studies focused on changes in CVC from rest *during* or *after* an orthostatic stressor. Moreover, all of these studies relied on bulky, wired electrocardiogram (ECG) and SBP recording setups for their analyses, which limit

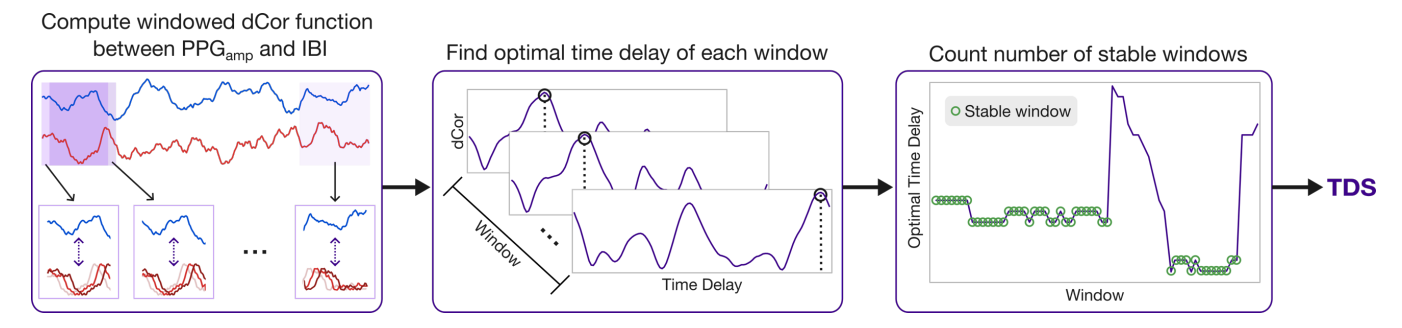


Fig. 2. Block diagram of methology for estimating the coupling between IBI and PPG_{amp} time series using TDS. IBI: interbeat interval; PPG_{amp}: PPG amplitude; dCor: distance correlation; TDS: time delay stability.

generalizability, especially in ambulatory settings. Therefore, there is a need to elucidate alterations in CVC before OH occurs, and to do so using more convenient sensing methods.

In prior work from our group, we demonstrated the utility of the CardioTag (Cardiosense, Chicago, IL, USA), a wireless, multimodal, chest-worn patch, in capturing cardiovascular responses that were predictive of OH in individuals with synucleinopathies [9], [10]. In this work, we applied a new analysis on this dataset by quantifying the coupling between cardiac and vascular function using time series features derived from the CardioTag. We found that those who experienced OH—induced by an orthostatic challenge—exhibited lower CVC during the supine rest period prior to the challenge than those who did not experience OH. To our knowledge, this is the first study to capture, during rest and prior to OH occurrence, an index of impaired CVC in those with OH using a compact, wearable patch. Our findings reinforce the effectiveness of wireless cardiovascular sensing technology for early screening and remote monitoring of CVAD using features derived from interactions between different signal modalities.

II. METHODS

A. Study Cohort and Protocol

We collected data from 26 participants, which included 20 individuals with synucleinopathies (13 with PD, 6 with MSA, 1 with DLB) and 6 healthy controls. During study recruitment, those with neurological conditions beyond PD, MSA or DLB or with a history of uncontrolled cardiovascular or psychiatric disorders were excluded. All participants completed a clinical protocol approved by the institutional review boards of the Georgia Institute of Technology (#H21492) and the Emory University School of Medicine (#00003055).

The orthostatic challenge protocol began by ensuring stabilization of supine hemodynamics with 5-15 minutes of supine rest. Then, each participant performed several autonomic testing maneuvers (e.g., paced breathing, Valsalva maneuver) in the supine position. Finally, each participant completed the active stand test by transitioning from supine to standing position and remaining upright for 5 minutes. In this work, we only analyzed the final 5 minutes of the supine rest and standing periods.

B. Physiological Sensing

During the orthostatic challenge protocol, we recorded cardiovascular activity using the CardioTag, which was affixed to the sternum with two standard gel electrodes and measured single-lead ECG and sternal photoplethysmogram (PPG) signals sampled at 500 Hz and 67 Hz, respectively. Additionally, we recorded non-invasive continuous blood pressure (CBP) as a reference measurement using one of two setups: 1) the ccNexfin (Edward Lifesciences, Irvine, CA, USA) or 2) the CNAP (CNSystems, Graz, Austria) along with the VS 9 (Mindray, Shenzhen, China). Beat-to-beat CBP was calibrated to minute-by-minute oscillometric brachial cuff blood pressure and heart rate recordings.

C. Cardiovascular Signal Processing and Feature Extraction

From the raw ECG and PPG signals during the supine period, we applied the signal processing pipeline described in detail in [9], which included bandpass filtering and fiducial point detection to extract interbeat interval (IBI) and PPG amplitude (PPG_{amp}) as time series indices of cardiac rhythm and blood volume pulsation, respectively. Additionally, we resampled and aligned each feature to 1 Hz using cubic spline interpolation. Finally, we smoothed each feature using a 5-second moving average filter to prevent the estimation of spurious interactions due to noise in the subsequent CVC quantification step.

D. Cardiovascular Coupling Estimation

To estimate the degree of coupling between IBI and PPG_{amp} during the 5-minute supine period, we applied a modified version of the time delay stability (TDS) analysis framework that was first presented in [11] (Fig. 2). First, we segmented each signal into sliding windows of length L shifted by s to form the sets $\{IBI^{(i)}\}_{i=1}^{N_L-1}$ and $\{PPG_{amp}^{(i)}\}_{i=1}^{N_L-1}$, where i denotes the window index and N_L denotes the total number of length-L windows across the full length each 5-minute signal. Next, we computed the time-varying distance correlation [12] function for each window as follows:

$$dCor^{i}(\tau) = \frac{dCov^{2}\left(PPG_{\rm amp}^{(i)}, IBI_{\tau}^{(i)}\right)}{\sqrt{dVar^{2}\left(PPG_{\rm amp}^{(i)}\right) \cdot dVar^{2}\left(IBI_{\tau}^{(i)}\right)}} \tag{1}$$

where $IBI_{\tau}^{(i)}$ is $IBI^{(i)}$ shifted by some delay τ , dVar is the distance variance, and dCov is the distance covariance, which is empirically computed (for some pair of vectors x and y) as follows:

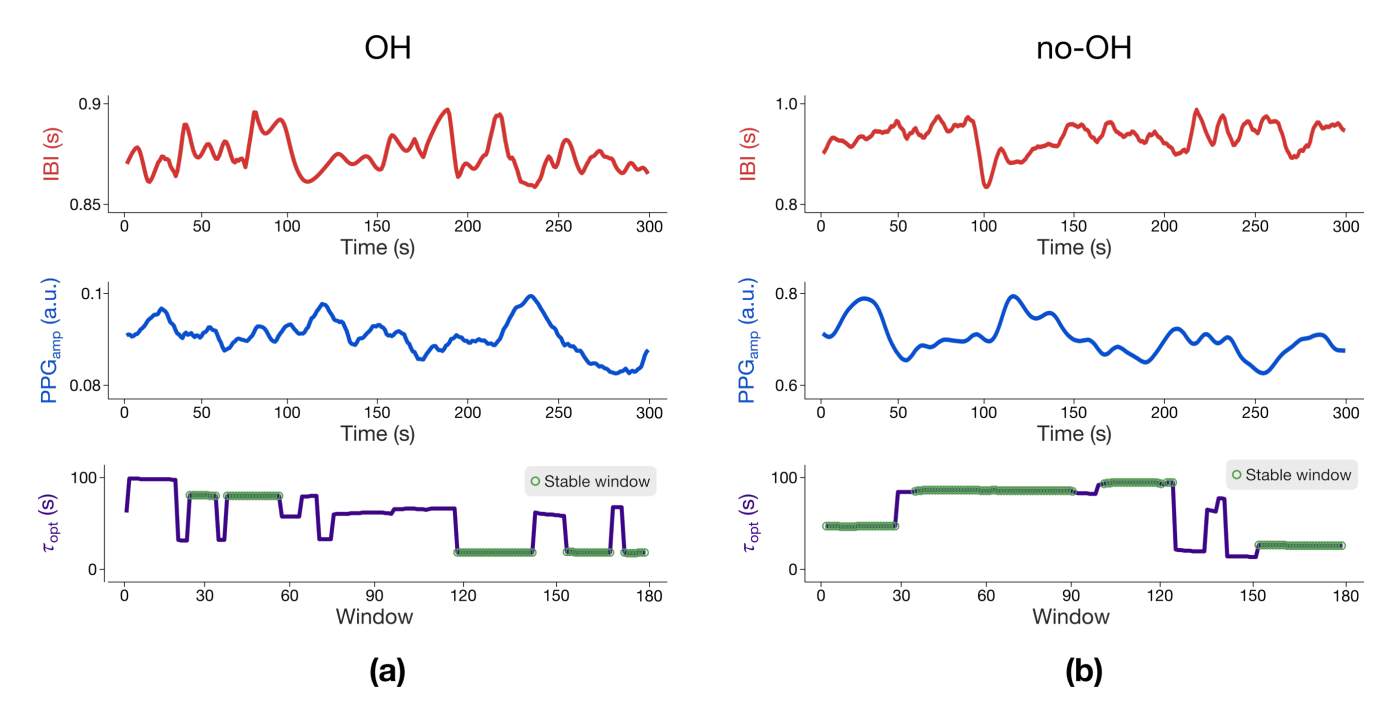


Fig. 3. Example IBI, PPG_{amp}, and $\tau_{\rm opt}$ signals during 5-minute supine rest from representative (a) OH participant and (b) no-OH participant. $\tau_{\rm opt}$ was computed as the time delay resulting in the maximal distance correlation between corresponding windows of IBI and PPG_{amp} signals of length L=120 seconds shifted by s=1 second. Stable windows were determined using T=30 seconds. IBI: interbeat interval; PPG_{amp}: PPG amplitude; $\tau_{\rm opt}$: optimal time delay.

$$dCov^{2}(x,y) = \frac{1}{n^{2}} \sum_{k,l=1}^{n} A_{kl} B_{kl}$$
 (2)

where A and B represent the Euclidean distance matrices of x and y, respectively. Furthermore, the distance variance of a vector x is computed as follows:

$$dVar^{2}(x) = dCov^{2}(x, x)$$
(3)

The computation in (1) presents a modification of the original TDS approach, which quantified the similarity between corresponding windows of two signals using the linear cross-correlation metric. To capture both linear interactions and any potential nonlinear interactions between the cardiovascular signals, we replaced the cross-correlation with the distance correlation function, which does not require substantial hyperparameter tuning like information-theoretic measures of dependence such as mutual information. From the distance correlation functions, we found the set of optimal time delays, i.e., the time delay that maximized (1) for each window i, as follows:

$$\tau_{opt}^{(i)} = \arg\max_{\tau} dCor^{(i)}(\tau)$$
 (3)

where $\left\{\tau_{opt}^{(i)}\right\}_{i=1}^{N_L}$ represents the set of optimal time delays for all N_L windows. Then, we followed the procedure outlined in [11] to count the number of "stable" windows, i.e., the number of windows that fall on an interval such that the optimal time delay of at least 0.8*T out of T consecutive windows are within ± 1 second of each other. Denoting the number of stable windows as N_T , we finally computed TDS_{CV} as

$$TDS_{CV}(\%) = \frac{N_T}{N_L} \times 100 \tag{4}$$

where CV denotes *cardiovascular*. Thus, TDS_{CV} quantifies the percentage of consecutive, overlapping length-L windows of cardiovascular signals whose optimal time delays agree. For our analysis, we chose L=120 seconds to ensure that we sufficiently captured meaningful variation in autonomic activity [13]. In accordance with Cai et al. [14], we chose M=1 to maximize the amount of data leveraged to evaluate TDS_{CV}, and we chose T=0.25L=30 for the stability requirement. Finally, as the focus of this work was to elucidate differences in CVC during rest and prior to OH occurrence, we only analyzed TDS_{CV} during supine rest. Example IBI and PPG_{amp} time series with optimal time delays derived via distance correlation are shown in Fig. 3.

E. OH vs. no-OH Comparisons

Using the reference beat-to-beat CBP measurements, we found that the orthostatic challenge protocol induced OH in 12 out of the 26 participants. After grouping participants by OH incidence and verifying normality and equal variances, we compared mean supine TDScv in the OH group vs. no-OH group using an independent t-test, and we computed Cohen's effect size, d, associated with the test. Then, to determine if TDScv during supine rest was correlated with the change in average systolic blood pressure (Δ SBP) induced by the orthostatic challenge, we ran both the Pearson and Spearman rank correlation tests. We set $\alpha = 0.05$ for all tests.

TABLE I: RESTING CARDIOVASCULAR COUPLING AND CHANGE IN SYSTOLIC BLOOD PRESSURE FOLLOWING ORTHOSTATIC TRANSITION

Group	Mean TDS _{CV} \pm SD	Mean ΔSBP ± SD
ОН	$30.1 \pm 16.3 \%$	-27.7 ± 21.3 mmHg
No-OH	53.0 ± 22.6 %	$10.1\pm15.8~\text{mmHg}$

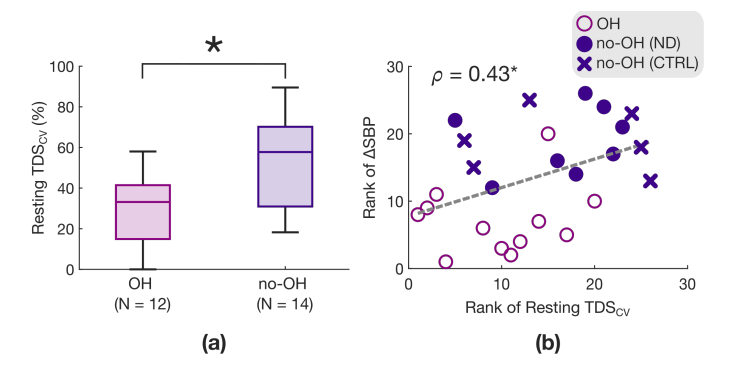


Fig. 4. Summary of cardiovascular coupling during supine rest in OH vs. no-OH across N=26 study participants. (a) Boxplots showing TDS between IBI and PPG_{amp} time series during supine rest in OH vs. no-OH participants. (b) Rank correlation plot between change in SBP from supine to standing and supine rest TDS_{CV}. (*) indicates statistically significant result (p < 0.05). OH: orthostatic hypotension; ND: neurodegenerative disease; CTRL: healthy control; TDS_{CV}: time delay stability between cardiovascular signals; IBI: interbeat interval; PPG_{amp}: PPG amplitude; SBP: systolic blood pressure; ρ : Spearman correlation coefficient.

III. RESULTS

TDS_{CV} and Δ SBP aggregated across each group is summarized in Table I. Mean supine TDS_{CV} was statistically significantly lower (t(24) = -2.92, p = 0.0076, d = -1.15) by 22.9% in the OH group compared to the no-OH group. Boxplots of TDS_{CV} for each group are shown in Fig. 4a. The Pearson correlation test revealed that Δ SBP and TDS_{CV} were not linearly correlated; however, according to the Spearman correlation test, TDS_{CV} and Δ SBP exhibited a moderate increasing monotonic relationship (Spearma's $\rho = 0.43$, p = 0.029). The Spearman rank correlation plot is shown in Fig. 4b.

IV. DISCUSSION AND CONCLUSION

The results from statistical testing demonstrate that in this study, those with OH following the orthostatic challenge were characterized by impaired coupling between IBI and PPG_{amp} at rest. These findings suggest that quantifying CVC using PPG signals recorded at the sternum may serve as a surrogate marker of BRS without the need for blood pressure measurement. Prior work from our lab found significant correlations between sternal PPGamp and changes in pulse pressure induced by a postural change from supine to standing [10] and that PPGderived pulse arrival time during supine rest significantly differed between no-OH and OH participants [9]. Thus, more broadly, findings from our prior work and from this study emphasize the utility of sternal PPG in conjunction with ECG for remotely estimating baroreflex function in the context of CVAD. To further validate our claims, future studies should apply the CVC analysis framework presented in this work to CardioTag data recorded in ambulatory settings.

In this work, we highlighted the effectiveness of a compact, multimodal chest-worn patch in capturing an index of resting-state CVC, and we demonstrated that this index was discriminative of the presence or absence of OH. Crucially, unlike prior studies in the literature, we identified impaired CVC more than 5 minutes before the occurrence of OH, and we

did not rely on a wired, bulky blood pressure sensing setup to estimate the coupling index. Our findings in this work, along with prior work from our lab, encourage the use of wearables for estimating continuous indices of baroreflex and autonomic function to enable remote detection of OH (or risk of OH onset) in individuals with neurodegenerative diseases associated with autonomic failure. These indices may assist clinicians in early detection and more optimal treatment of CVAD in the future.

V. DISCLOSURES

O. T. Inan is a co-founder and board member of Cardiosense, Inc., the company that manufactures CardioTag, and has equity ownership in that company. He also holds equity in Physiowave and Biozen.

REFERENCES

- M. Metzler, S. Duerr, R. Granata, F. Krismer, D. Robertson, and G. K. Wenning, "Neurogenic orthostatic hypotension: pathophysiology, evaluation, and management," *J Neurol*, vol. 260, no. 9, pp. 2212–2219, Sep. 2013
- [2] A. Fedorowski and O. Melander, "Syndromes of orthostatic intolerance: a hidden danger," *Journal of Internal Medicine*, vol. 273, no. 4, pp. 322–335, 2013.
- [3] J. G. Bradley and K. A. Davis, "Orthostatic hypotension," Am Fam Physician, vol. 68, no. 12, pp. 2393–2398, Dec. 2003.
- [4] K. H. Masaki et al., "Orthostatic Hypotension Predicts Mortality in Elderly Men," Circulation, vol. 98, no. 21, pp. 2290–2295, Nov. 1998.
- [5] P. A. Low and V. A. Tomalia, "Orthostatic Hypotension: Mechanisms, Causes, Management," *J Clin Neurol*, vol. 11, no. 3, pp. 220–226, Jul. 2015.
- [6] S. Charleston-Villalobos et al., "Time-Frequency Analysis of Cardiovascular and Cardiorespiratory Interactions During Orthostatic Stress by Extended Partial Directed Coherence," Entropy, vol. 21, no. 5, Art. no. 5, May 2019.
- [7] S. Reulecke et al., "Study of impaired cardiovascular and respiratory coupling during orthostatic stress based on joint symbolic dynamics," Medical Engineering & Physics, vol. 61, pp. 51–60, Nov. 2018.
- [8] A. Marchi et al., "Evaluation of the correlation between cardiac and sympathetic baroreflex sensitivity before orthostatic syncope," in 2015 37th Annual International Conference of the IEEE Engineering in Medicine and Biology Society (EMBC), Aug. 2015, pp. 2063–2066.
- [9] J. A. Berkebile et al., "Remote Monitoring of Cardiovascular Autonomic Dysfunction in Synucleinopathies With a Wearable Chest Patch," *IEEE Sensors Journal*, vol. 25, no. 4, pp. 7250–7262, Feb. 2025.
- [10] J. A. Berkebile, O. T. Inan, and P. A. Beach, "Evaluating Orthostatic Responses with Wearable Chest-Based Photoplethysmography in Patients with Parkinson's Disease," in 2023 IEEE SENSORS, Oct. 2023, pp. 1–4.
- [11] A. Bashan, R. P. Bartsch, J. W. Kantelhardt, S. Havlin, and P. C. Ivanov, "Network physiology reveals relations between network topology and physiological function," *Nat Commun*, vol. 3, no. 1, p. 702, Feb. 2012.
- [12] G. J. Székely, M. L. Rizzo, and N. K. Bakirov, "Measuring and testing dependence by correlation of distances," *The Annals of Statistics*, vol. 35, no. 6, pp. 2769–2794, Dec. 2007.
- [13] T. F. of the E. S. of C. the N. A. S. of P. Electrophysiology, "Heart Rate Variability," *Circulation*, vol. 93, no. 5, pp. 1043–1065, Mar. 1996.
- [14] Z. Cai, H. Gao, M. Wu, J. Li, and C. Liu, "Physiologic Network-Based Brain-Heart Interaction Quantification During Visual Emotional Elicitation," *IEEE Transactions on Neural Systems and Rehabilitation Engineering*, vol. 32, pp. 2482–2491, 2024.